Spectral Latent Heating (SLH) for GPM

Algorithm Theoretical Basis Document (ATBD)

Algorithm Ver. 07A

Prepared by
GPM SLH Algorithm Development Team

December 2021

TABLE OF CONTENTS

1. General Summary for Spectral Latent Heating (SLH) 1
1.1. Retrieval for the Tropics 2
1.2. Retrieval for mid latitudes 3
1.3. Retrieval for great mountain ranges in the tropical precipitation regime 9
2. I/O data description 12
2.1. Overview 12
2.2. L2 product (LHP for TRMM and SLP for GPM) 13
2.2.1. Input data for LHP/SLP 13
2.2.2. Output data for LHP/SLP 13
2.3. L3 products (LHG for TRMM and SLG for GPM) 17
2.3.1. Input data for LHG/SLG 17
2.3.2. Output data for LHG/SLG 17
2.4. L3 products (LHM for TRMM and SLM for GPM) 20
2.4.1. Input variables for LHM/SLM 20
2.4.2. Output data for LHM/SLM 21
3. REFERENCES 24

1. General Summary for Spectral Latent Heating (SLH)

Convective latent heating plays essential roles for tropical convection, generating mesoscale circulations (e.g. Houze et al. 1989). Moreover, vertical profiles of diabatic heating, in which convective latent heating contributes largely, affects the general circulation of the atmosphere (e.g. Hartmann et al. 1984). For mid-latitude systems also, latent heating contributes to generations of PVs resulting in, for example, explosive intensifications of mid-latitude storms (Boettcher and Wernli, 2011).

Previously, with TRMM PR V7A, we developed SLH latent heating algorithm (Shige, Takayabu et al. 2004, 2007, etc) for tropical and subtropical TRMM observation region (35N-35S). With GPM DPR, the observation region extended to 65N-65S. Now we are to modify our latent heating retrieval algorithm (SLH) to be applicable from the tropics to mid-latitudes.

For GPM SLH V05 algorithm, we retrieve latent heating variables utilizing two separate algorithms for tropics and for mid-latitudes. First, location of each GPM KuPR pixel is assigned to either tropics or mid-latitudes, depending on monthly maps of precipitation types determined in a similar manner as described in Takayabu (2008). Then, we retrieve three dimensional latent heating (LH), Q1-QR (Q1R), and Q2, applying either tropical/mid-latitude algorithms to precipitation data observed from GPM DPR (KuPR). Here, Q1 and Q2 are apparent heat source and apparent moisture sink, respectively, introduced by Yanai et al. (1973), and QR is radiative heating of the atmosphere.

For TRMM V8A/ GPM V06A algorithm, the SLH algorithm and Tables are the same as GPM SLH V5 for mid-latitude and TRMM SLH V7A for tropics. However, the input PR/KuPR Level 2 data was changed.

After the release of the SLH V06A product, we found an issue that the revision of its input data KuPR level 2, which increased the stratiform precipitation, also increased a gap between near-surface precipitation observed by the KuPR and vertically integrated latent heating retrieved by the SLH algorithm. Besides, some unnatural heating profiles were found around tropical cyclones. To fix these problems, we revised the algorithm to release the SLH V06B product.

For TRMM/GPM V07 product, we develop a new algorithm for great mountain ranges in the tropical precipitation regime. The areas of the great mountain ranges in the tropical precipitation regime are assigned based on the monthly maps of precipitation types used for tropical/mid-latitude algorithms and elevation. Note only LH is retrieved for great mountain ranges in the tropical precipitation regime in the TRMM/GPM SLH V07 product. In following subsections, we briefly describe the Spectral Latent Heating (SLH) algorithms for tropics, for mid-latitude precipitation, and great mountain ranges in the tropical precipitation regime.

1.1. Retrieval for the Tropics

With the TRMM PR, we first developed the spectral latent heating (SLH) algorithm for the tropics as summarized in Fig.1, in a following manner. First, utilizing the Goddard Cumulus Ensemble Model, we simulated the TOGA-COARE precipitation, from which we made three spectral look-up tables (LUTs) of latent heating profiles in terms of precipitation top height (PTH) for convective rain and melting level precipitation rate (MLP) for deep stratiform rain. Utilizing TRMM PR precipitation profiles and these tables, we estimated the latent heating associated with the precipitation. Please refer to Shige et al. (2004, 2007, 2008, and 2009) for details. Heating in all shallow pixels with their precipitation top heights (threshold 0.3mm/hr) lower than the melting level is estimated as convective type (rainTypeSLH=11). A LUT for shallow stratiform rain is only used for other rain (rainTypeSLH=61) in the SLH V07 algorithm.

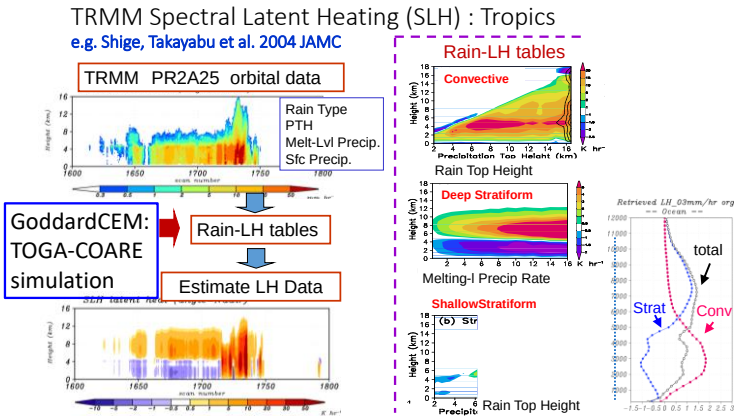

Fig.1: Summary of the SLH for tropics.

Deep stratiform rain is now further divided into two new categories: deep stratiform with decreasing precipitation from the melting level toward the surface (rainTypeSLH=31) and deep stratiform with increasing precipitation from the melting level toward the surface (rainTypeSLH=32). The SLH algorithm computes deep stratiform cooling magnitudes as a function of the precipitation rate at the melting level (Pm) – the precipitation rate at near surface (Pnsfc), assuming the evaporative cooling rate below the melting level in deep stratiform regions is proportional to the reduction in the precipitation profile toward the surface from the melting level (based on 1D water substance conservation). However, increasing precipitation profiles are found in some portions of stratiform regions, especially in regions adjacent to convective regions where 1D water substance conservation may be invalid. LH for the intermediary pixels is retrieved

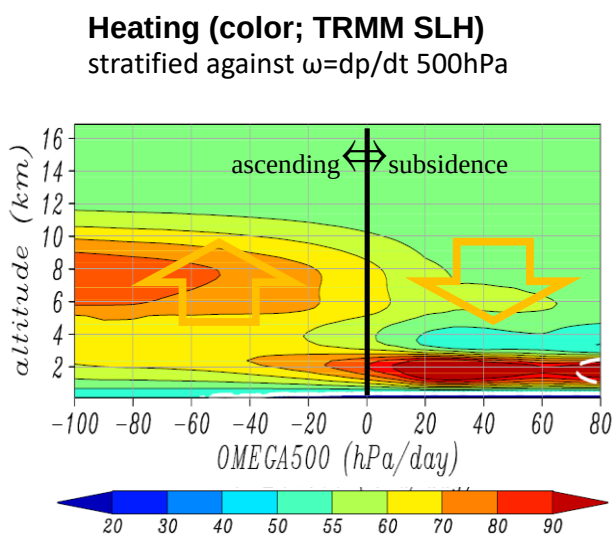

Fig.2: SLH-estimated Q1-QR profiles in 30N-30S at all longitudes over oceans, stratified with pressure velocity at 500hPa. Congestus regime is found in the large-scale subsidence region with Q1R peak at around 2km.

with the deep stratiform LUT but without cooling below the melting level. This retrieval method is based on the consideration that cooling below the melting level is unrealistic under the condition which produces downward-increasing precipitation below the melting level.

Utilizing these TRMM SLH, we found an existence of clear congestus regime with relatively high sea surface temperature with suppressed deep convection associated with large-scale atmospheric subsidence (Fig. 2). It was connected to solve the double ITCZ problem that climate model developers have long been plagued (Hirota et al. 2011).

1.2. Retrieval for mid latitudes

For mid-latitude systems, we employ the Japan Meteorological Agency (JMA)'s high resolution (horizontally 2km) local forecast model (LFM) to construct the LUTs. With collaborations of JMA's forecast group, 3hr and 4hr forecast data for 8 extratropical cyclone cases (16 shots) are collected and utilized for LUTs.

In treating mid-latitude systems, in contrast to the tropical systems, we first faced a "cloud base problem". In a tropical Mesoscale Convective System (MCS), we basically assume that freezing level coincides with its cloud base level for its stratiform precipitation area. For mid latitude stratiform precipitation, however, this assumption does not hold.

LH is closely related to various phase changes of water. Figure 3 shows the LH profiles associated with various phase change processes. Left panel is an example, where cloud base is below freezing level, melting and condensation occur at similar levels, and they cancel each other. While, when cloud base is above the freezing level, evaporation and melting occur together and result in a large cooling. So, we really need cloud base level information. But we only observe radar reflectivity profiles for precipitation with GPM DPR. Here, we tried to obtain the cloud base information from the precipitation profiles.

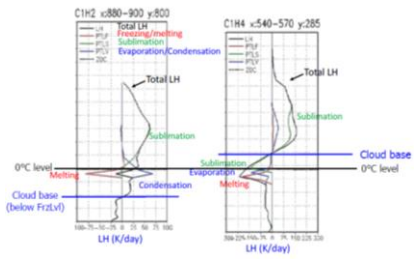

Fig.3: Latent heating associated with cloud processes for cloud base level below the freezing level case (left) and cloud base level above the freezing level (right).

Since precipitation should evaporate out of the cloud base, we may expect that precipitation maximum level (Pmax) can represent the cloud base. Figure 4 scatter the precipitation maximum heights against cloud base heights for stratiform precipitation: Downward Decreasing (DD) precipitation from the 0degC level, Downward Increasing (DI) precipitation, and others.

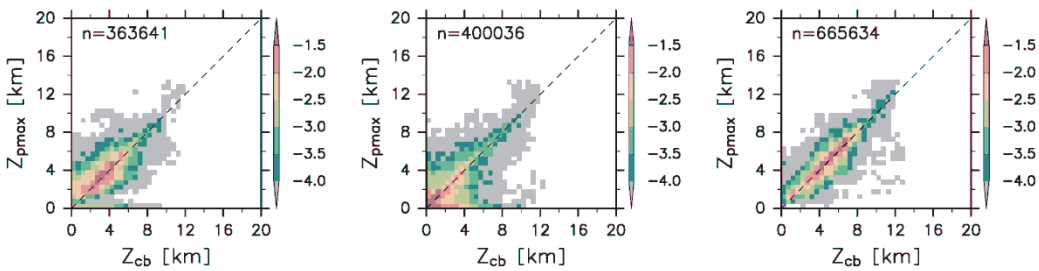

Fig. 4: Scatter histograms between cloud base levels (Zcb) and maximum precipitation heights (Zpmax). For DD, DI

and other stratiform precipitation.

Finally, LUTs for the six precipitation types (convective, shallow stratiform, 3 types of deep stratiform, and other) were constructed for LH, Q1R, and Q2. The deep stratiform tables are further divided according to whether maximum precipitation (Pmax) exists above the surface or at the surface. These nine types of LUTs for LH are shown in Fig. 5. Convective and shallow stratiform tables are made against the precipitation top heights. Ordinate is the altitudes, and color shades are LH profiles for each bin. For deep stratiform and other precipitation, LUT are made against maximum precipitation (Pmax) chosen for the abscissa. In these LUTs, ordinate is the standardized altitude with zero at the Pmax level, and +1.0 and -1.0 correspond to PTH and the precipitation bottom height (PBH), respectively.

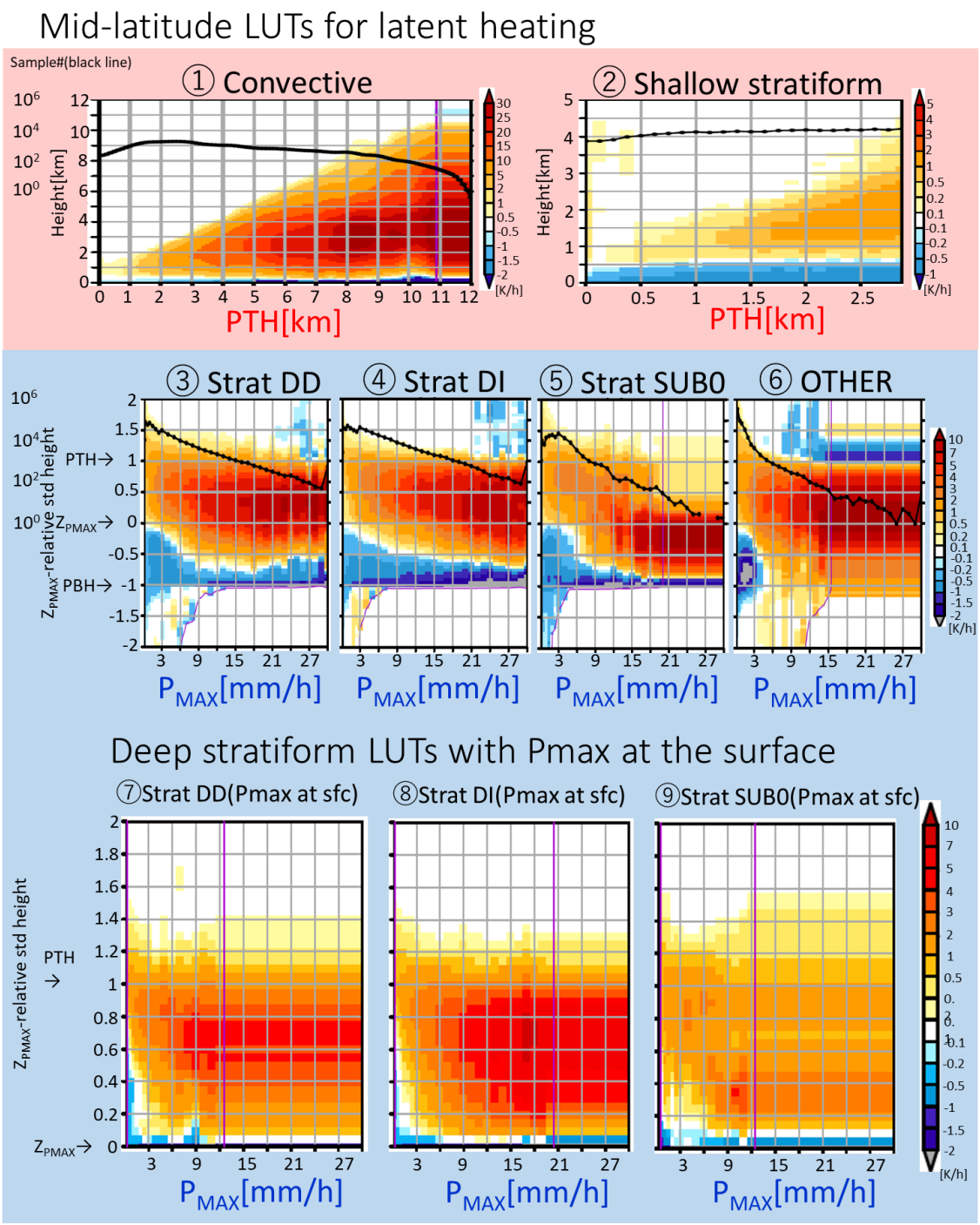

Fig.5: LUTs constructed from 8 extratropical cyclone cases simulated by JMA LFM. See text for details.

Utilizing the nine LUTs and precipitation profile data from GPM 2AKu, LH is retrieved. Precipitation type (convective/ stratiform/ other), PTH, PBH, Pmax, and Pnsfc are utilized for input.

In order to see the performance of the retrieval, we first performed a consistency check. We compared LH retrieved from model precipitation and Model simulated LH along the red line of Fig. 6. Results are shown in Fig. 7. Left panels show the cross sections for precipitation, simulated LH and retrieved LH from top to bottom. We can confirm that retrieved LH looks very similar to

simulated LH. Right panel show the averaged profiles for simulated LH in black and retrieved LH in red curves. Examining each section separately (Fig. 8), we can confirm successful reconstruction of LH by this algorithm.

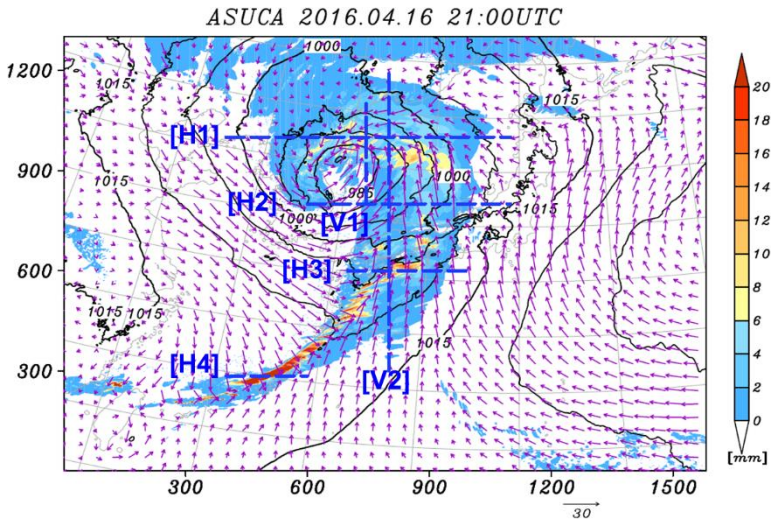

Fig. 6: LFM-simulated precipitation for extratropical cyclone case 1.

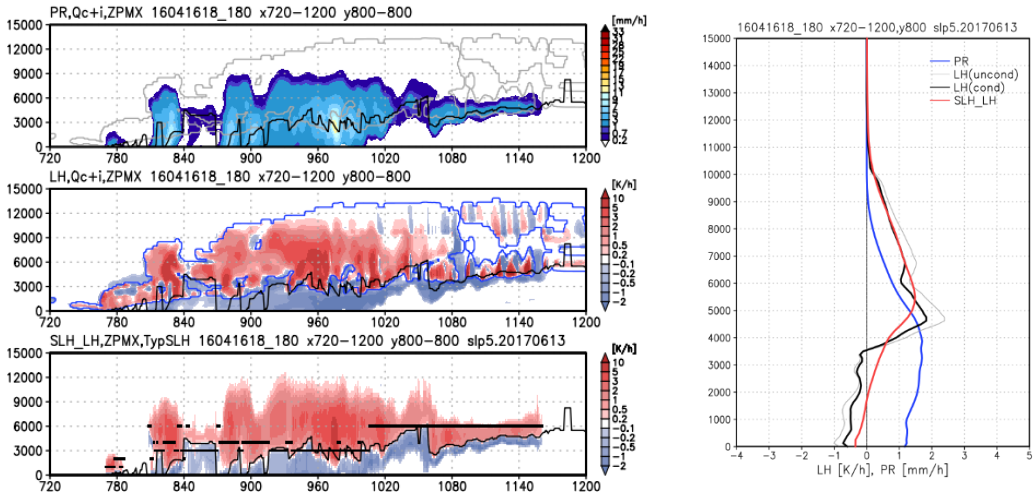

Fig. 7: Left: Precipitation, simulated LH, and SLH-retrieved LH using simulated precipitation, from top to bottom, respectively. Right: Averaged (in x-dir) profiles of precipitation (blue), simulated LH (black) and retrieved LH (red).

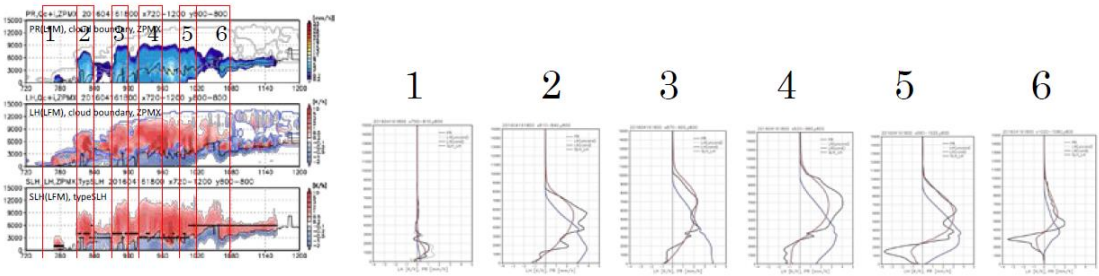

Fig. 8: Same as Fig.5 but the profiles are averaged for separate parts of the system numbered 1-6.

Finally, GPM KuPR is utilized for the retrieval. The left panels show precipitation and precipitation types from GPM KuPR. Note that there is no guarantee that the simulation corresponds well to the observation along a satellite orbit. But it seems to be a marvelous simulation (Fig.9).

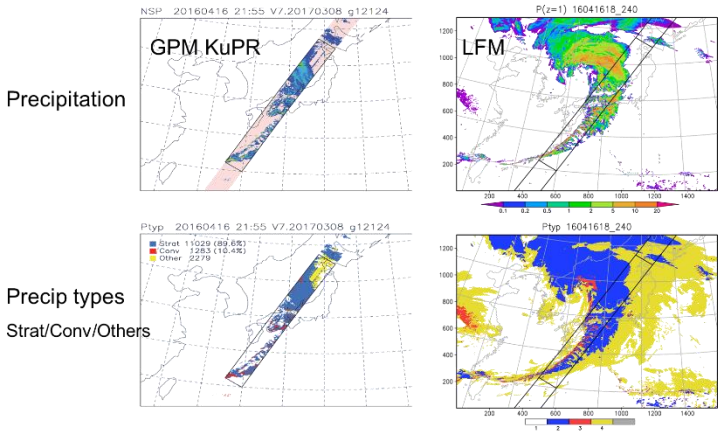

Fig. 9: Upper panels: GPM-observed precipitation and LFM-simulated precipitation at 18z 16Apr, 2016 (4hrF). Lower panels: Precipitation types

Figure 10 compare simulated and retrieved LH along the GPM orbit. Left panels are LFM-simulated precipitation and LH, middle are LFM precipitation and retrieved LH from LFM precipitation, Right panels show GPM-precipitation and retrieved LH. Precipitation simulation is very good, so we can compare these cross sections. The retrieval looks quite successful.

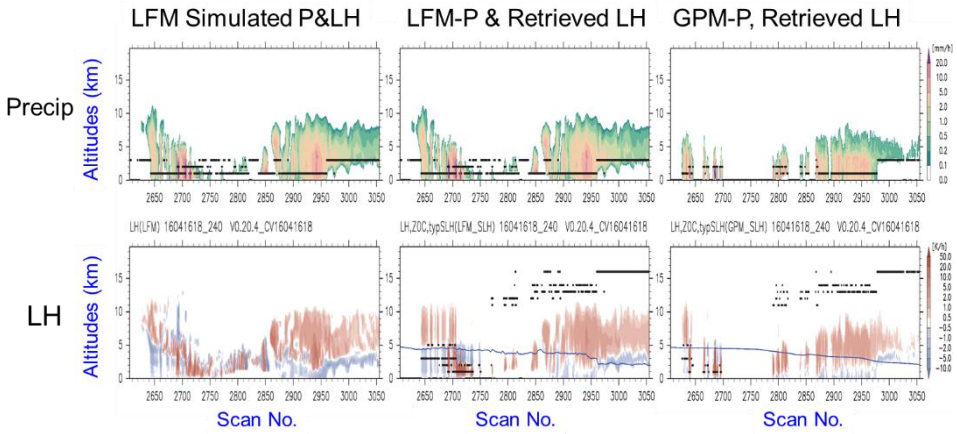

Fig. 10: Simulated and (LFM- & GPM-) retrieved LH along the GPM orbit shown in Fig. 9.

Finally, average profiles of LH are compared for eight cases (Fig. 11). Red dashed are GPM retrieved profiles and Black is LFM-simulated LH, for total, convective, stratiform, and others. They are surprisingly consistent. Excellent correspondences are confirmed for cases with reasonable precipitation coverages (cases 1, 3, 5, 6, 8) in the evaluation regions of GPM swaths.

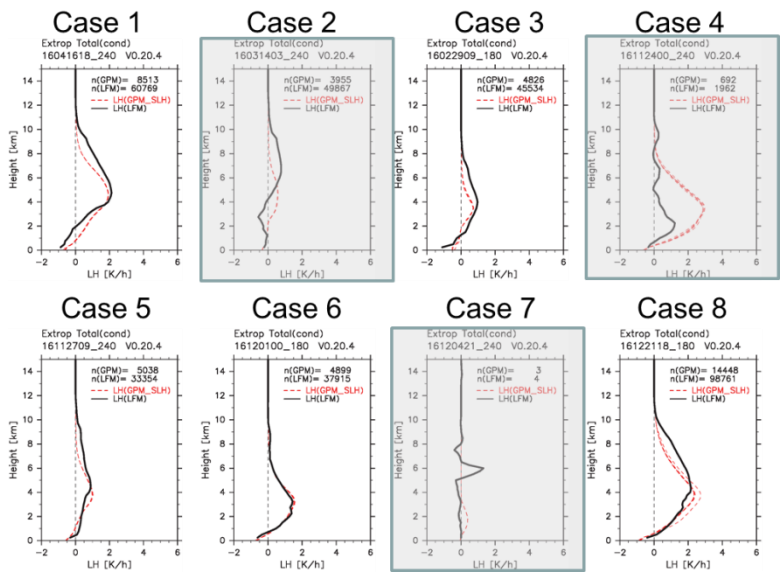

Fig. 11: Evaluations of GPM-retrieved LH for 8 cases. Red dotted curves represent retrieved GPM LH, and black curves are for simulated LH. Cases with mid-lat precipitation coverage are inefficient for evaluations are covered with gray shades.

We also confirmed a good continuities of LH distributions between tropics and midlatitudes in horizontal maps (Fig. 12) as well as in zonal mean vertical structure.

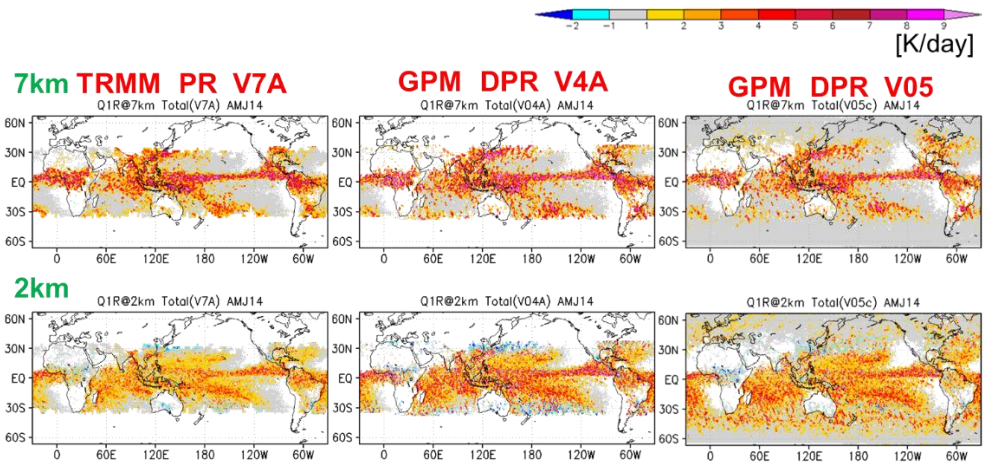

Fig. 12: Horizontal distributions of LH derived with GPM SLH V5 algorithm.

The LUTs are constructed with data collected at each grid individually from the LFM simulation with the precipitation intensity exceeding 0.2 mm h^{-1}. Although small frozen hydrometeors can fall as precipitation after being advected by large-scale flow associated with extratropical cyclones, as shown schematically in Fig. 13, the LUTs does not consider LH related to such advected small hydrometeors. Therefore, vertically integrated LH is probably smaller than near-surface precipitation over GPM observation areas.

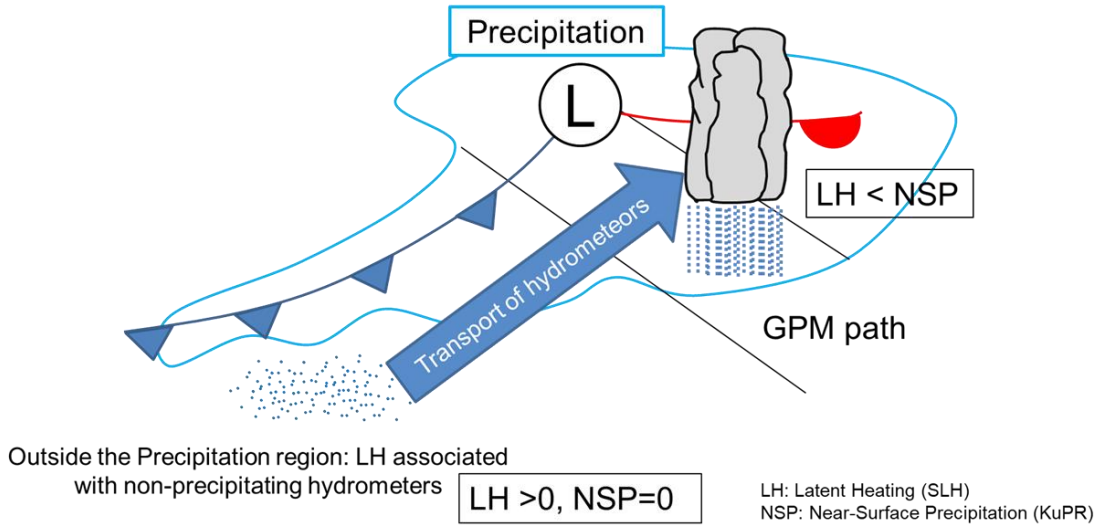

Fig. 13: Schematic figure showing small hydrometeors advected by large-scale flow.

To consider LH associated with such small hydrometeors, LH associated with generations of such small hydrometeors is estimated by the LFM simulation output and is added to correct the LH retrieved with the LUT. The additional LH is calculated in a following manner: At first, two types of sum of vertically integrated LH, namely LHt and LHp, are calculated for each snapshot of the simulations (8 cases, 16 snapshots). LHp is the sum of vertically integrated LH at the precipitating grids in which the precipitation regime is midlatitude ocean, whereas LHt is the sum of vertically integrated LH at all grids in which the precipitation regime is midlatitude ocean. Then, the ratio between LHp and LHt, LHp/LHt, is calculated for each snapshot. The average of the ratio from 16 snapshots turns out to be 0.88. Finally, the LH retrieved from the original SLH algorithm is corrected by dividing by the value “0.88”. This correction factor is named as ‘correctionFactorMidLatType’.

The application of this factor in the orbital products is inconsistent in terms of pixel-by-pixel estimation. Therefore, this factor is not applied to SLP and SLG products but applied to SLM products. The specific value of the correctionFactorMidLatType is stored in the AlgorithmRuntimeInfo in the SLP product and “correctionFactorMidLatType” in the SLM product.

To summarize, we developed a new Spectral LH algorithm for mid-latitude precipitation, utilizing 8 extratropical cyclone cases simulated with JMA LFM. To this end, cloud Base vs Freezing Level relationship was an issue, for we utilize precipitation profiles observed from the GPM KuPR.

We found that precipitation maximum height can well represent the cloud base height. Nine LUTs were constructed to retrieve LH from GPM KuPR. This new algorithm performed successfully: Consistency check and retrieval results were quite satisfactory.

1.3. Retrieval for great mountain ranges in the tropical precipitation regime

For great mountain ranges in the tropical precipitation regime, the LUTs are newly developed using the Weather Research and Forecasting (WRF) model. Two cases observed by the GPM KuPR during summer are simulated, one over the Tibetan Plateau and the other on the slopes around the

Tibetan Plateau. The areas of the great mountain ranges in the tropical precipitation regime are shown in Figure 14.

The great mountain range module shares a common algorithm framework of the midlatitude module described in Sec 1.2. However, since the topography needs to be considered, there are some differences. For convective and shallow stratiform rain, the LUTs are separately produced depending on whether the elevation is higher or lower than 4 km (Fig. 15a-d), because of differences in the vertical distribution of heating. For deep stratiform, the LUTs are not separately produced depending on the elevation, but SUB0 (where the 0°C level appears near the surface) deep stratiform categories (Fig. 15i, j) are mainly for deep stratiform precipitation over high elevations and other deep stratiform categories (Fig. 15e-h) for deep stratiform precipitation over low elevations. The LUT for OTHER category is not produced and the LUTs for shallow and deep stratiform are applied for other type.

As a result, the ten LUTs are produced for the great mountain range module (the nine LUTs for the midlatitude module): 1. convection over high elevations (Fig. 15a), 2. convection over low elevations (Fig. 15b), 3. shallow stratiform over high elevations (Fig. 15c), 4. shallow stratiform over low elevations (Fig. 15d), 5. downward increasing (DI) deep stratiform with maximum precipitation (Pmax) aloft (Fig. 15e), 6. DI deep stratiform with Pmax near the surface (Fig. 15f), 7. downward decreasing (DD) deep stratiform with Pmax aloft (Fig. 15g), 8. DD deep stratiform with Pmax near the surface (Fig. 15h), 9. SUB0 (where the 0°C level appears near the surface) deep stratiform with Pmax aloft (Fig. 15i), and 10. SUB0 deep stratiform with Pmax near the surface (Fig. 15j).

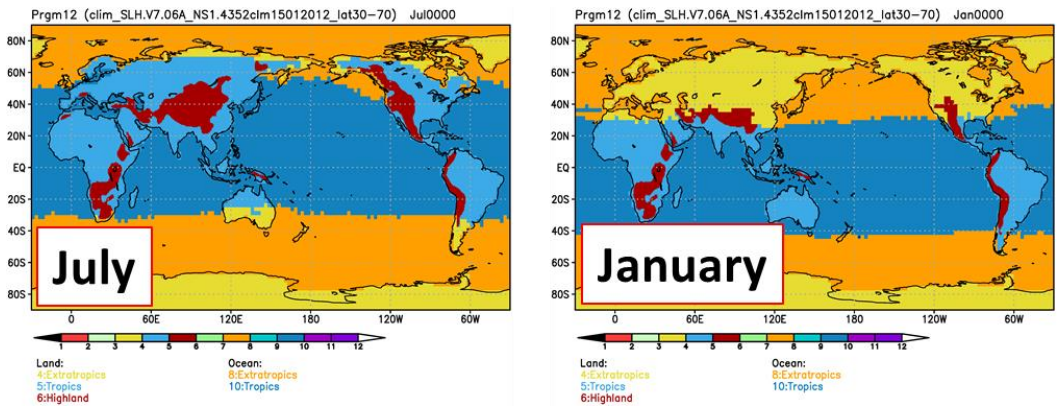

Fig. 14 Distribution of the areas of the great mountain ranges in the tropical precipitation regime (6: Highland) with those of tropics (5: Tropics over Land and 10: Tropics over Ocean) and mid and higher latitudes (4: Extratropics over Land and 8: Extratropics over Ocean) for July (left) and January (right).

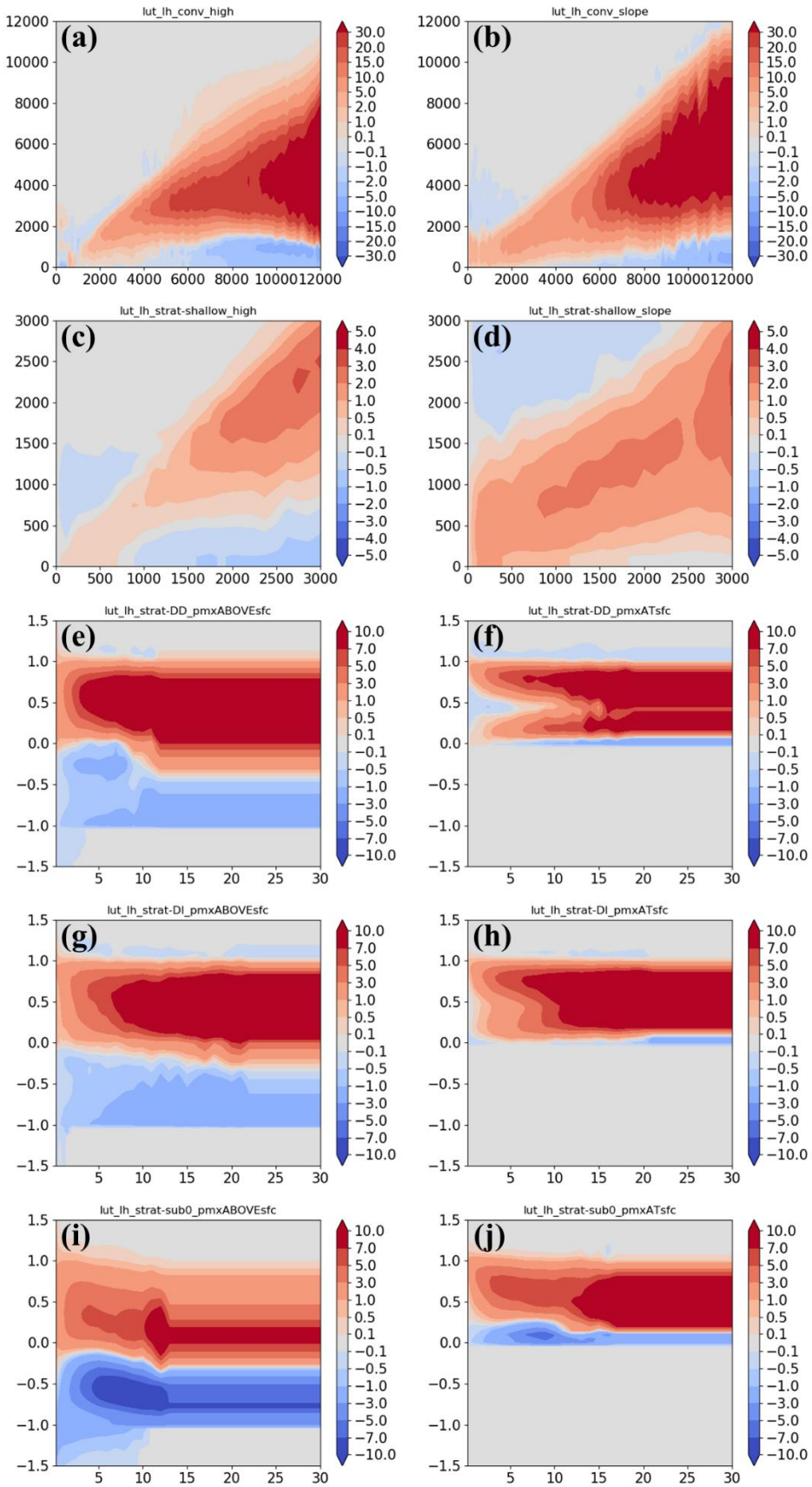

Fig. 15 LUTs for great mountain ranges in the tropical precipitation regime. See text for details.

2. I/O data description

2.1. Overview

TRMM/GPM-SLH level-2 algorithm uses 2APR/2AKu product as input. Followings are summary of PR and KuPR. L2 algorithm also uses a precipitation regime database as an auxiliary data. TRMM/GPM-SLH level-3 algorithms use LHP/SLP product as input.

Table 1 Major specification of TRMM/PR and GPM/KuPR

Satellite	Height (km)	Instrument	frequency (GHz)	Data Period
TRMM	350 (November 1997–August 2001) 402 (August 2001-April 2015)	PR	13.8	November 1997–April 2015
GPM Core Observatory	407	KuPR	13.6	March 2014–present

As for output data, we provide LHP/SLP and LHM/SLM. Table 2 shows the brief description for them.

Table 2. Description for GPM SLH products

Products	Level	Descriptions	Temporal resolution	Horizontal resolution	Vertical resolution	Coverage	Output format
LHP/SLP	L2	Basic orbital SLH.	-	5km	80 layers*	-	HDF5 formats
LHG/SLG	L3	Gridded orbital SLH.	path	0.5-degree latitude/longitude grid.		180°W to 180°E/, 67°S to 67°N.	
LHM/SLM		Monthly averaged SLH	monthly				

* at the fixed height of 0.00-0.25 km, 0.25-0.50 km0.0-0.5km, 0.5-1.0km, ..., 19.50-19.75 km, and 19.75-20.00 km.

It should be noted that conditional mean values were added to L3 product from TRMM/GPM Version 06A, and variable names for L3 product were changed from TRMM/V7A and GPM/V05A. Detail is explained in following subsections.

[Note about the missing value conditions]

Note that there are two reasons for missing values for conditional mean (LHCndMean, Q1RCndMean, Q2CndMean), which can be discriminated by 'allPix' values as follows.

1. conditional mean is not defined because there is no precipitation in the grid (precipPix=0), when allPix≠0.

2. missing value is given because the grid value is masked out related to the topography, when and allPix = 0.

[Note about CorrectionFactorMidLatType in SLM]

After the SLH V06B algorithm, heating (LH, Q1R, Q2) has been corrected by the CorrectionFactorMidLatType=0.88 in the area where the midlatitude algorithm is applied. In V07, because this factor is changed to be applied to only the SLM product, but not to the SLP product, the monthly mean of the L2 heating divided by the factor corresponds to the SLM product in the midlatitude area.

2.2. L2 product (LHP for TRMM and SLP for GPM)

2.2.1. Input data for LHP/SLP

LHP and SLP products are generated by using the following variables from 2APR/2AKu products as input data:

scanStatus/dataQuality
scanTime
Latitude
Longitude
PRE/binClutterFreeBottom
PRE/binRealSurface
PRE/flagPrecip
PRE/landSurfaceType
PRE/localZenithAngle
VER/heightZeroDeg
CSF/typePrecip
SLV/binEchoBottom
SLV/precipRate
SLV/zFactorCorrected

2.2.2. Output data for LHP/SLP

2.2.2.1. Dimension Definition

- nscan
  - var Number of scans in the granule.
- nray
  - 49 Number of angle bins in each scan
- nlayer
  - 80 Number of layers at the fixed height of 0.00-0.25 km, 0.25-0.50 km, ..., 19.50-19.75 km, and 19.75-20.00 km.

2.2.2.2. Output variables

ScanTime/Year (2-byte integer, size: nscan)

4-digit year. Missing value is −9999.

ScanTime/Month (1-byte integer, size: nscan)

Month of the year. Missing value is −9999.

ScanTime/DayOfMonth (1-byte integer, size: nscan)

Day of the month. Missing value is −9999.

ScanTime/Hour (1-byte integer, size: nscan)

UTC hour of the day. Missing value is −9999.

ScanTime/Minute (1-byte integer, size: nscan)

Minute of the hour. Missing value is −9999.

ScanTime/Second (1-byte integer, size: nscan)

Second of the minute. Missing value is −9999.

ScanTime/MilliSecond (2-byte integer, size: nscan)

Thousandths of the second. Missing value is −9999.

ScanTime/DayOfYear (2-byte integer, size: nscan)

Day of the year. Missing value is −9999.

ScanTime/SecondOfDay (4-byte float, size: nscan)

Second of the day. Missing value is −9999.

Latitude (4-byte float, size: nray x nscan)

Latitude of the pixel center. Positive north, negative south. Missing value is −9999.9.

Longitude (4-byte float, size: nray x nscan)

Longitude of the pixel center. Positive east, negative west. Missing value is −9999.9.

latentHeating (4-byte float, size: nlayer x nray x nscan)

Latent heating. Unit is [K/h]. Missing value is −9999.9.

Q1minusQR (4-byte float, size: nlayer x nray x nscan)

Apparent heat source minus radiative heating rate; Q1-QR. Unit is [K/h]. Missing value is −9999.9. Q1R is missing in V07A when rainTypeSLH is for great mountain ranges in the tropical

precipitation regime (rainTypeSLH=200-268)

Q2 (4-byte float, size: nlayer x nray x nscan)

Apparent moisture sink Q2. Unit is [K/h]. Missing value is −9999.9. Q2 is missing in V07A when rainTypeSLH is for great mountain ranges in the tropical precipitation regime (rainTypeSLH=200-268)

rainTypeSLH (2-byte integer, size: nray x nscan)

Precipitation type decided by SLH algorithm. The values are listed below.

Table 3. Description for rainTypeSLH

(a) Tropics and subtropics	(b) Mid and higher latitudes	(c) Great mountain ranges in the tropical precipitation regime
0: No precipitation	100: No precipitation	200: No precipitation
11: Convective	111: Convective	211: Convective over high-elevation areas 212: Convective over low-elevation areas
21: Shallow stratiform	121: Shallow stratiform	221: Shallow stratiform over high-elevation areas 222: Shallow stratiform over low-elevation areas
31: Deep stratiform 32: Deep stratiform, DI (Intermediary)	131: Deep stratiform, DD, Pmax aloft 132: Deep stratiform, DD, Pmax NS 133: Deep stratiform, DI, Pmax aloft 134: Deep stratiform, DI, Pmax NS 135: Deep stratiform, subzero, Pmax aloft 136: Deep stratiform, subzero, Pmax NS	231: Deep stratiform, DD, Pmax aloft 232: Deep stratiform, DD, Pmax NS 233: Deep stratiform, DI, Pmax aloft 234: Deep stratiform, DI, Pmax NS 235: Deep stratiform, subzero, Pmax aloft 236: Deep stratiform, subzero, Pmax NS
61: Other, Applying table for rainTypeSLH=21	160: Other	261: Other, Applying table for rainTypeSLH=221 262: Other, Applying table for rainTypeSLH=222 263: Other, Applying table for rainTypeSLH=231 264: Other, Applying table for rainTypeSLH=232 265: Other, Applying table for rainTypeSLH=233 266: Other, Applying table for rainTypeSLH=234 267: Other, Applying table for rainTypeSLH=235 268: Other, Applying table for rainTypeSLH=236
Mask		
900: Areas with low melting levels including some mountains except for of great mountain ranges in the tropical precipitation regime 910: Suspicious extreme 920: No precipitation in SLH (precipRate < 0.2 mm/h (0.3 mm/h for tropics) or precipitation depth < 500m) but precipitation exists in 2Aku		

DI: Downward Increasing, DD: Downward Decreasing, NS: Near Surface

rainType2APR/rainType2ADPR (2-byte integer, size: nray x nscan)

Precipitation type copied from 2AKu or 2APR. Missing value is −9999.

surfaceType (2-byte integer, size: nray x nscan)

Land surface type. The values are;

0: Ocean, 1: Land, 2: Cost, 3: Inland water, and missing value is −9999.

stormTopHeight (2-byte integer, size: nray x nscan)

For tropical types, height of storm top. For midlatitude types and great mountain range types, precipitation-top height of the lowest precipitation layer. Unit is [m]. Missing value is −9999.

nearMeltLevel (2-byte integer, size: nray x nscan)

Height with maximum precipitation rate around the heightZeroDeg level when rainTypeSLH is 31 (Deep stratiform), or height of surface level when rainTypeSLH is 32 (Deep stratiform with low melting level). All missing for midlatitude types, great mountain range types and other tropical types. Unit is [m]. Missing value is −9999.

nearSurfLevel (2-byte integer, size: nray x nscan)

For tropical types, height of the clutter free bottom. For midlatitude types and great mountain range types, precipitation-bottom height of the lowest precipitation layer. Unit is [m]. Missing value is −9999.

topoLevel (2-byte integer, size: nray x nscan)

Height of topography estimated from binRealSurface and localZenithAngle in 2AKu. Unit is [m]. Missing value is −9999.

meltLevel (2-byte integer, size: nray x nscan)

Melting level defined as a height of the closest SLH bin to the heightZeroDeg in 2AKu. Unit is [m]. Missing value is −9999.

levelConvUpper (2-byte integer, size: nray x nscan)

For tropical convective types with high storm top height, height 500-m higher from the height at closest SLH bin to the heightZeroDeg in 2AKu except for precipitation profiles with maximum well above the heightZeroDeg. All missing for midlatitude types and great mountain range types. Unit is [m]. Missing value is −9999.

nearSurfPrecipRate (4-byte float, size: nray x nscan)

For tropical types, precipitation rate at the near-surface level. For midlatitude types and great mountain range types, precipitation rate at the bottom level of the lowest precipitation layer. Unit is [mm/h]. Missing value is −9999.9.

precipRateNearMelt (4-byte float, size: nray x nscan)

For tropical deep stratiform types, precipitation rate at nearMeltLevel. All missing for midlatitude types and great mountain ranges types. Unit is [mm/h]. Missing value is −9999.9.

precipRateConvUpper (4-byte float, size: nray x nscan)

For tropical convective types with high storm top height, precipitation rate at the levelConvUpper to determine the upper-level heating due to ice process. All missing for midlatitude types and great mountain range types. Unit is [mm/h]. Missing value is −9999.9.

2.3. L3 products (LHG for TRMM and SLG for GPM)

2.3.1. Input data for LHG/SLG

LHG and SLG (orbit-based gridded) products are generated by using the following variables from LHP/SLP products as input data:

Swath/Latitude
Swath/Longitude
Swath/Q1minusQR
Swath/Q2
Swath/ScanTime/DayOfMonth
Swath/ScanTime/DayOfYear
Swath/ScanTime/Hour
Swath/ScanTime/MilliSecond
Swath/ScanTime/Minute
Swath/ScanTime/Month
Swath/ScanTime/Second
Swath/ScanTime/Year
Swath/latentHeating
Swath/rainType2APR (for TRMM)
Swath/rainType2ADPR (for GPM)

2.3.2. Output data for LHG/SLG

2.3.2.1. Dimension Definition

- nlat
  - 268 number of high resolution 0.5° grid intervals of latitude from 67°S to 67°N.
- nlon
  - 720 number of high resolution 0.5° grid intervals of longitude from 180°W to 180°E.
- nlayer
  - 80 number of layers at the fixed heights of 0.00-0.25 km, 0.25-0.50 km, ..., 19.50-19.75 km, and 19.75-20.00 km.

2.3.2.2. Output variables

GridTime/Year (2-byte integer, size: nscan)

4-digit year. Missing value is -9999.

GridTime/Month (1-byte integer, size: nscan)

Month of the year. Missing value is -99.

GridTime/DayOfMonth (1-byte integer, size: nscan)

Day of the month. Missing value is -99.

GridTime/Hour (1-byte integer, size: nscan)
UTC hour of the day. Missing value is -99.

GridTime/Minute (1-byte integer, size: nscan)
Minute of the hour. Missing value is -99.

GridTime/Second (1-byte integer, size: nscan)
Second of the minute. Missing value is -99.

GridTime/MilliSecond (2-byte integer, size: nscan)
Thousandths of the second. Missing value is -9999.

GridTime/DayOfYear (2-byte integer, size: nscan)
Day of the year. Missing value is -9999.

allLHCndMean (4-byte float, size: nlat x nlon x nlayer)
All Conditional mean of latent heating. Unit is [K/h]. Missing value is -9999.9.

allLHUnCndMean (4-byte float, size: nlat x nlon x nlayer)
All Unconditional mean of latent heating . Unit is [K/h]. Missing value is -9999.9.

allPix (2-byte integer, size: nlat x nlon x nlayer)
All pixel counts. Missing value is -9999.9.

allQ1RCndMean (4-byte float, size: nlat x nlon x nlayer)
All Conditional mean of Q_1-Q_R. Unit is [K/h]. Missing value is -9999.9.

allQ1RUnCndMean (4-byte float, size: nlat x nlon x nlayer)
All Unconditional mean of Q_1-Q_R. Unit is [K/h]. Missing value is -9999.9.

allQ2CndMean (4-byte float, size: nlat x nlon x nlayer)
All Conditional mean of Q_2. Unit is [K/h]. Missing value is -9999.9.

allQ2UnCndMean (4-byte float, size: nlat x nlon x nlayer)
All Unconditional mean of Q_2. Unit is [K/h]. Missing value is -9999.9.

convLHCndMean (4-byte float, size: nlat x nlon x nlayer)
Conditional mean of convective latent heating. Unit is [K/h]. Missing value is -9999.9.

convPix (2-byte integer, size: nlat x nlon x nlayer)
Convective pixel counts. Missing value is -9999.9.

convQ1RCndMean (4-byte float, size: nlat x nlon x nlayer)
Conditional mean of convective Q_1-Q_R. Unit is [K/h]. Missing value is -9999.9.

convQ2CndMean (4-byte float, size: nlat x nlon x nlayer)
Conditional mean of convective Q_2. Unit is [K/h]. Missing value is -9999.9.

dpstrLHCndMean (4-byte float, size: nlat x nlon x nlayer)
Conditional mean of stratiform latent heating. Unit is [K/h]. Missing value is -9999.9.

dpstrPix (2-byte integer, size: nlat x nlon x nlayer)
Stratiform pixel counts. Missing value is -9999.9.

dpstrQ1RCndMean (4-byte float, size: nlat x nlon x nlayer)
Conditional mean of stratiform Q_1-Q_R. Unit is [K/h]. Missing value is -9999.9.

dpstrQ2CndMean (4-byte float, size: nlat x nlon x nlayer)
Conditional mean of stratiform Q_2. Unit is [K/h]. Missing value is -9999.9.

otherLHCndMean (4-byte float, size: nlat x nlon x nlayer)
Conditional mean of other latent heating. Unit is [K/h]. Missing value is -9999.9.

otherPix (2-byte integer, size: nlat x nlon x nlayer)
Other pixel counts. Missing value is -9999.9.

otherQ1RCndMean (4-byte float, size: nlat x nlon x nlayer)
Conditional mean of other Q_1-Q_R. Unit is [K/h]. Missing value is -9999.9.

otherQ2CndMean (4-byte float, size: nlat x nlon x nlayer)
Conditional mean of other Q_2. Unit is [K/h]. Missing value is -9999.9.

precipPix (2-byte integer, size: nlat x nlon x nlayer)
Precipitation pixel counts. Missing value is -9999.9.

shstrLHCndMean (4-byte float, size: nlat x nlon x nlayer)
Conditional mean of shallow-stratiform latent heating. Unit is [K/h]. Missing value is -9999.9.

shstrPix (2-byte integer, size: nlat x nlon x nlayer)

Shallow-stratiform pixel counts. Missing value is -9999.9.

shstrQ1RCndMean (4-byte float, size: nlat x nlon x nlayer)

Conditional mean of shallow-stratiform Q_1-Q_R. Unit is [K/h]. Missing value is -9999.9.

shstrQ2CndMean (4-byte float, size: nlat x nlon x nlayer)

Conditional mean of shallow-stratiform Q_2. Unit is [K/h]. Missing value is -9999.9.

2.4. L3 products (LHM for TRMM and SLM for GPM)

2.4.1. Input variables for LHM/SLM

LHM and SLM (Monthly) products are generated by using the following variables from daily products calculating from SLP/LHP (intermediate product called LHD/SLD, not distributed) as input data:

Grid/LHCndMean
Grid/LHCndStdv
Grid/Q1RCndMean
Grid/Q1RCndStdv
Grid/Q2CndMean
Grid/Q2CndStdv
Grid/allPix
Grid/convLHCndMean
Grid/convLHCndStdv
Grid/convPix
Grid/convQ1RCndMean
Grid/convQ1RCndStdv
Grid/convQ2CndMean
Grid/convQ2CndStdv
Grid/dpstrLHCndMean
Grid/dpstrLHCndStdv
Grid/dpstrPix
Grid/dpstrQ1RCndMean
Grid/dpstrQ1RCndStdv
Grid/dpstrQ2CndMean
Grid/dpstrQ2CndStdv
Grid/otherLHCndMean
Grid/otherLHCndStdv
Grid/otherPix
Grid/otherQ1RCndMean

Grid/otherQ1RCndStdv
Grid/otherQ2CndMean
Grid/otherQ2CndStdv
Grid/precipPix
Grid/shstrLHCndMean
Grid/shstrLHCndStdv
Grid/shstrPix
Grid/shstrQ1RCndMean
Grid/shstrQ1RCndStdv
Grid/shstrQ2CndMean
Grid/shstrQ2CndStdv

2.4.2. Output data for LHM/SLM

2.4.2.1. Dimension Definition

- nlat
  - 268 number of high resolution 0.5° grid intervals of latitude from 67°S to 67°N.
- nlon
  - 720 number of high resolution 0.5° grid intervals of longitude from 180°W to 180°E.
- nlayer
  - 80 number of layers at the fixed heights of 0.00-0.25 km, 0.25-0.50 km, ..., 19.50-19.75 km, and 19.75-20.00 km.

2.4.2.2. Output variables

LHCndMean (4-byte float, size: nlat x nlon x nlayer)

Conditional mean of latent heating. Unit is [K/h]. Missing value is -9999.9.

LHCndStdv (4-byte float, size: nlat x nlon x nlayer)

Conditional standard deviation of latent heating. Unit is [K/h]. Missing value is -9999.9.

LHUnCndMean (4-byte float, size: nlat x nlon x nlayer)

Unconditional mean of latent heating. Unit is [K/h]. Missing value is -9999.9.

LHUnCndStdv (4-byte float, size: nlat x nlon x nlayer)

Unconditional standard deviation of latent heating. Unit is [K/h]. Missing value is -9999.9.

Q1RCndMean (4-byte float, size: nlat x nlon x nlayer)

Conditional mean of Q_1-Q_R. Unit is [K/h]. Missing value is -9999.9.

Q1RCndStdv (4-byte float, size: nlat x nlon x nlayer)

Conditional standard deviation of Q_1-Q_R. Unit is [K/h]. Missing value is -9999.9.

Q1RUnCndMean (4-byte float, size: nlat x nlon x nlayer)
Unconditional mean of Q_1-Q_R. Unit is [K/h]. Missing value is -9999.9.

Q1RUnCndStdv (4-byte float, size: nlat x nlon x nlayer)
Unconditional standard deviation of Q_1-Q_R. Unit is [K/h]. Missing value is -9999.9.

Q2CndMean (4-byte float, size: nlat x nlon x nlayer)
Conditional mean of Q_2. Unit is [K/h]. Missing value is -9999.9.

Q2CndStdv (4-byte float, size: nlat x nlon x nlayer)
Conditional standard deviation of Q_2. Unit is [K/h]. Missing value is -9999.9.

Q2UnCndMean (4-byte float, size: nlat x nlon x nlayer)
Unconditional mean of Q_2. Unit is [K/h]. Missing value is -9999.9.

Q2UnCndStdv (4-byte float, size: nlat x nlon x nlayer)
Unconditional standard deviation of Q_2. Unit is [K/h]. Missing value is -9999.9.

allPix (4-byte float, size: nlat x nlon x nlayer)
All pixel counts. Missing value is -9999.9.

convLHCndMean (4-byte float, size: nlat x nlon x nlayer)
Conditional mean of convective latent heating. Unit is [K/h]. Missing value is -9999.9.

convLHCndStdv (4-byte float, size: nlat x nlon x nlayer)
Conditional standard deviation of convective latent heating. Unit is [K/h]. Missing value is -9999.9.

convPix (4-byte float, size: nlat x nlon x nlayer)
Convective pixel counts. Missing value is -9999.9.

convQ1RCndMean (4-byte float, size: nlat x nlon x nlayer)
Conditional mean of convective Q_1-Q_R. Unit is [K/h]. Missing value is -9999.9.

convQ1RCndStdv (4-byte float, size: nlat x nlon x nlayer)
Conditional standard deviation of convective Q_1-Q_R. Unit is [K/h]. Missing value is -9999.9.

convQ2CndMean (4-byte float, size: nlat x nlon x nlayer)

Conditional mean of convective Q_2. Unit is [K/h]. Missing value is -9999.9.

convQ2CndStdv (4-byte float, size: nlat x nlon x nlayer)
Conditional standard deviation of convective Q_2. Unit is [K/h]. Missing value is -9999.9.

dpstrLHCndMean (4-byte float, size: nlat x nlon x nlayer)
Conditional mean of stratiform latent heating. Unit is [K/h]. Missing value is -9999.9.

dpstrLHCndStdv (4-byte float, size: nlat x nlon x nlayer)
Conditional standard deviation of stratiform latent heating. Unit is [K/h]. Missing value is -9999.9.

dpstrPix (4-byte float, size: nlat x nlon x nlayer)
Stratiform pixel counts. Missing value is -9999.9.

dpstrQ1RCndMean (4-byte float, size: nlat x nlon x nlayer)
Conditional mean of stratiform Q_1-Q_R. Unit is [K/h]. Missing value is -9999.9.

dpstrQ1RCndStdv (4-byte float, size: nlat x nlon x nlayer)
Conditional standard deviation of stratiform Q_1-Q_R. Unit is [K/h]. Missing value is -9999.9.

dpstrQ2CndMean (4-byte float, size: nlat x nlon x nlayer)
Conditional mean of stratiform Q_2. Unit is [K/h]. Missing value is -9999.9.

dpstrQ2CndStdv (4-byte float, size: nlat x nlon x nlayer)
Conditional standard deviation of stratiform Q_2. Unit is [K/h]. Missing value is -9999.9.

otherLHCndMean (4-byte float, size: nlat x nlon x nlayer)
Conditional mean of other latent heating. Unit is [K/h]. Missing value is -9999.9.

otherLHCndStdv (4-byte float, size: nlat x nlon x nlayer)
Conditional standard deviation of other latent heating. Unit is [K/h]. Missing value is -9999.9.

otherPix (4-byte float, size: nlat x nlon x nlayer)
Other pixel counts. Missing value is -9999.9.

otherQ1RCndMean (4-byte float, size: nlat x nlon x nlayer)
Conditional mean of other Q_1-Q_R. Unit is [K/h]. Missing value is -9999.9.

otherQ1RCndStdv (4-byte float, size: nlat x nlon x nlayer)
Conditional standard deviation of other Q_1-Q_R. Unit is [K/h]. Missing value is -9999.9.

otherQ2CndMean (4-byte float, size: nlat x nlon x nlayer)
Conditional mean of other Q_2. Unit is [K/h]. Missing value is -9999.9.

otherQ2CndStdv (4-byte float, size: nlat x nlon x nlayer)
Conditional standard deviation of other Q_2. Unit is [K/h]. Missing value is -9999.9.

shstrLHCndMean (4-byte float, size: nlat x nlon x nlayer)
Conditional mean of shallow-stratiform latent heating. Unit is [K/h]. Missing value is -9999.9.

shstrLHCndStdv (4-byte float, size: nlat x nlon x nlayer)
Conditional standard deviation of shallow-stratiform latent heating. Unit is [K/h]. Missing value is -9999.9.

shstrPix (4-byte float, size: nlat x nlon x nlayer)
Shallow-stratiform pixel counts. Missing value is -9999.9.

shstrQ1RCndMean (4-byte float, size: nlat x nlon x nlayer)
Conditional mean of shallow-stratiform Q_1-Q_R. Unit is [K/h]. Missing value is -9999.9.

shstrQ1RCndStdv (4-byte float, size: nlat x nlon x nlayer)
Conditional standard deviation of Q_1-Q_R. Unit is [K/h]. Missing value is -9999.9.

shstrQ2CndMean (4-byte float, size: nlat x nlon x nlayer)
Conditional mean of shallow-stratiform Q_2. Unit is [K/h]. Missing value is -9999.9.

shstrQ2CndStdv (4-byte float, size: nlat x nlon x nlayer)
Conditional standard deviation of shallow-stratiform Q_2. Unit is [K/h]. Missing value is -9999.9.

correctionFactorMidLatType (4-byte float, scalar)
A correction factor to consider the effect of hydrometeors condensed outside and transported into the precipitating area. This factor is applied to mid latitude module and details are described in Fig. 13 and related explanations in section 1.2.

3. REFERENCES

Boettcher, M., and H. Wernli, 2011: Life Cycle Study of a Diabatic Rossby Wave as a Precursor to Rapid Cyclogenesis in the North Atlantic—Dynamics and Forecast Performance. Mon. Wea. Rev., 139, 1861-1878.

Hartmann, D. L., H. H. Hendon, and R. A. Houze, Jr., 1984: Some implications of the mesoscale circulations in tropical cloud clusters for large-scale dynamics and climate. J. Atmos. Sci., 41, 113-121.

Hirota, N., Y. N. Takayabu, M. Watanabe, M. Kimoto, 2011: Precipitation reproducibility over tropical oceans and its relationship to the double ITCZ problem in CMIP3 and MIROC5 climate models. *J. Climate*, **7**, 4859-4873.

Houze, R. A., Jr., S. A. Rutledge, M. I. Biggerstaff, and B. F. Smull, 1989: Interpretation of Doppler weather radar displays of midlatitude mesoscale convective systems. Bull. Amer. Meteor. Soc., 70, 608-619.

Shige, S., Y. N. Takayabu, W.-K. Tao, and D. E. Johnson, 2004: Spectral retrieval of latent heating profiles from TRMM PR data. Part I: Development of a model-based algorithm. *J. Appl. Meteor.*, **43**, 1095-1113.

Shige, S., Y. N. Takayabu, W.-K. Tao, and C.-L. Shie, 2007: Spectral retrieval of latent heating profiles from TRMM PR data. Part II: Algorithm improvement and heating estimates over tropical ocean regions. *J. Appl. Meteor. Climatol.*, **46**, 1098-1124.

Shige, S., Y. N. Takayabu, and W.-K. Tao, 2008: Spectral retrieval of latent heating profiles from TRMM PR data. Part III: Estimating apparent moisture sink profiles over tropical oceans. *J. Appl. Meteor. Climatol.*, **47**, 620-640.

Shige, S., Y. N. Takayabu, S. Kida, W.-K. Tao, X. Zeng, C. Yokoyama, and T. L'Ecuyer, 2009: Spectral retrieval of latent heating profiles from TRMM PR data. Part IV: Comparisons of lookup tables from two- and three-dimensional cloud-resolving model simulations. *J. Climate*, **22**, 5577-5594.

Takayabu, Y. N., 2008: Observing Rainfall Regimes Using TRMM PR and LIS Data, GEWEX News, vol.8 No.2, p.1,9-10.

Takayabu,Y. N., S. Shige, W.-K. Tao, and N. Hirota, 2010: Shallow and deep latent heating modes over tropical oceans observed with TRMM PR spectral latent heating data. *J. Climate*, **23**, 2030-2046.

Yanai, M., S. Esbensen and J. Chu, 1973: Determination of average bulk properties of tropical cloud clusters from large-scale heat and moisture budgets. J. Atmos. Sci., 30, 611-627.